Available online at www.sciencedirect.com
SciVerse ScienceDirect
Energy Procedia 24 (2012) 194 – 201
Energy Procedia

DeepWind, 19-20 January 2012, Trondheim, Norway

Structural design and analysis of a 10MW wind turbine blade

Kevin Cox[a], Andreas Echtermeyer[b],a*

[a,b]Norwegian University of Science and Technology, Richard Birkelandsvei 2B, Trondheim 7491, Norway

Abstract

The structural aspects of a 70 meter long blade in an upwind, horizontal-axis wind turbine were developed in this paper for use in a high wind speed location. A hybrid composite structure using glass and carbon fiber plies was created yielding a light-weight design with a low tip deflection. The blade was subjected to FEA studies to demonstrate its ability to withstand the extreme loading conditions as defined in the international offshore wind standard. The results confirmed the design to have acceptable performance with regard to tip deflection, maximum and minimum strains, and critical buckling load. Detailed descriptions of the structural components and ply layups are presented along with the resulting maximum and minimum strains and deflections. In addition, optimization techniques were introduced to provide insight for future studies with the blade.

Keywords:Wind turbine blade; FEA; Composite; Buckling

1. Introduction

Wind turbines have begun moving from land installations to offshore locations in an effort to harness the faster and steadier winds that exist there. When moving turbines offshore, the trend is to increase the rotor diameter so that more of this steady wind can be captured, ultimately decreasing the cost of energy. This increase in diameter creates design issues for many of the components, with the blade length being the first parameter affected. Little information is publically available on the structural design process of multi-megawatt blades since it is kept confidential by most manufacturers. Thus, there is a need for large scale reference blades that are openly available for research projects. In this study, a detailed blade model was developed and analyzed with respect to industry standard failure criteria to specify the structural components and the composite ply layups of the blade.

* Corresponding author. Tel.: +47-735-925-39; fax: +47-735-941-29.
E-mail address: kevin.cox@ntnu.no.

 doi:10.1016/j.egypro.2012.06.101

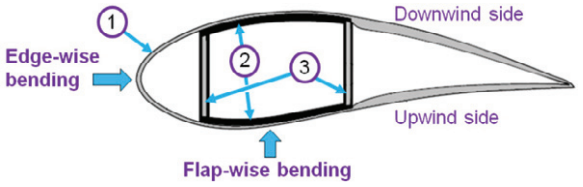

Figure 1: Cross section of a blade with references to the airfoil shell, spar flanges, and shear webs: #s 1, 2, and 3 respectively.

2. Blade Design

The structural design process of the wind turbine blade is constrained mainly by the aerodynamic outer surface of the blade and required stiffness criteria. Because the aerodynamics of the blade were not the focus of this study, the 10MW blade profile defined in [1] was used. The aerodynamic shell of this 70 meter blade was designed using blade element momentum theory and utilized the same airfoil families as those in the NREL 5 MW turbine [2]. The blade shape and length as well as information on the design parameters (found on page 2 of [1]) provided a starting point for developing the structural definition.

There are typically three members contributing to the stiffness of the blade so that it is able to resist the various loads. In addition to capturing the wind and converting it into torque, the airfoil shell provides the blade with stiffness to resist torsional and edgewise bending loads. Flapwise bending is the most significant load subjected to the blade and is resisted by utilizing a thick section of stiff composite material on the upwind and downwind sides of the airfoil. These stiffened sections are termed spar flanges and are connected by shear webs. The shear webs provide some torsional and edgewise bending stiffness but mainly contribute to shear stiffness. Fig. 1 depicts a common blade cross-section.

The regions between the shear webs locate the sections of high bending stiffness (the spar flanges). The webs are generally placed at 15% and 50% of the airfoil chord length so that the spar flanges are in the regions farthest from the neutral bending axis, thus providing the maximum amount of bending stiffness [3]. The distance between the webs determines the width of the spar flanges, again affecting the bending stiffness.

3. Material Selection

Blades currently used in industry for large turbines are composed of fiber composite materials so that a stiff, lightweight design with a high fatigue life is achieved. The fibers for wind turbine blades are typically oriented to 0^o, $+45^o$, and -45^o orientations, with 0^o being parallel to the blade span direction, or pitching axis. Plies with 0^o fibers are used for resisting bending while plies with $\pm 45^o$ fibers are implemented for torsional stiffness and buckling resistance [4]. Other combinations of fiber directions can be used, but the $0/\pm 45$ ply layup is the most practical from a manufacturing point of view. The material properties used in this study are presented in Table 1.

This study used the common assumptions that composite layups are very thin when compared with the structure's cross section, and that only in-plane (with respect to the laminate surface) loads are applied to the structure. Thus, since all out-of plane stresses and strains were assumed zero, and the thin structures do not exhibit through-thickness shear, only the in plane properties were required.

Many papers have studied incorporation of carbon fiber into large blades and have found possibilities for improved performance and even lower cost than using only glass fiber [3], [5], and [6]. As is common in these references, carbon fiber is best used as a replacement for the 0^o glass fibers in the spar flanges, yielding a lower tip deflection, higher buckling resistance, and lighter weight than an all glass layup. Therefore, this method was also utilized in this study.

Table 1: Material properties

Material	E_{xx} (GPa)	E_{yy} (GPa)	G_{xy} (GPa)	υ_{xy}	ρ (kg/m^3)	Ply thickness (mm)
0^o Carbon [5]	139.0	9.0	5.50	0.32	1560	2.0
0^o Glass [5]	41.0	9.0	4.10	0.30	1890	1.0
Core [7]	0.25	0.25	0.073	0.35	200	5.0
Lining [3]	9.65	9.65	3.86	0.30	1670	0.38
Gel Coat [3]	3.44	3.44	1.38	0.30	1230	0.51

Implementing a core material into a composite layup is a light-weight method to increase buckling resistance. The core material in Table 1 was chosen for its low weight and high shear modulus which is important for sandwich structures subjected to bending. This material was applied in all regions except for the spar flanges and the airfoil shell regions overlaying the flanges.

The lining is a thin composite layer with short, randomly oriented fibers used as a protective layer for the glass, carbon, and core ply layups. Finally, the gel coat was used as the outermost layer on the airfoil skin to create a smooth, aerodynamic surface for the blade.

4. FEA Preprocessing

The blade geometry was modeled in SolidWorks with 8 airfoil cross-section profiles as defined in Fig. 1 of [1], with the 1st cross-section being the circular section where the blade exits the hub. Each airfoil section was located along the pitching axis and rotated to the angles specified in Table 4 of [1]. The shear webs were located at 15% and 50% along the length of each airfoil chord (except near the root) and were twisted to remain perpendicular to the chord along the blade span. The 8 profiles were connected with the Shell Loft feature which created parabolic tangencies between the profiles to provide a smooth, continuous surface [8]. The root section, located inside the turbine hub, was not included in this study because hub connection was outside the scope of this work.

The shell geometry was imported into ABAQUS and split into 38 sections along the length as shown in Figure 2 (a) for finite element preprocessing and analysis. The large number of sections allowed for a well defined distribution of composite plies and aerodynamic point loads. It was then meshed using the ABAQUS S4R element: a 4-node, doubly curved element with reduced integration and hourglass control, appropriate for thick or thin shell applications [9]. Mesh convergence studies yielded a meshing technique with 12 elements across the spar flanges and 5 across the shear webs, as shown in Fig. 2 (b). 16 elements were used along the leading region of the airfoil (the fore side of the spar), and 6 on each side of the regions aft of the spar. The number of elements in the cross-section remained constant along the blade span, while their lengths ranged from 0.344 m at section 1 to 0.052 m at section 38.

5. Load Cases

Section 1 of Figure 2 (a) was fully constrained and point loads were applied to the 4 vertices of the spar cross-section numbers 2 – 39 to simulate the flapwise, edgewise, and torsional loads experienced by the blade. These were based on the assumption that the center of pressure was located at ¼ of the chord length from the leading edge. The point forces were specified to follow the nodal rotations during the analysis, thus yielding conservative results. The magnitudes and directions of the point loads were calculated from IEC load conditions in [1] using the aeroelastic software FAST by NREL.

From the load cases studied in [1], the most severe (largest tip deflections) were the extreme operating gust (EOG) at the rated wind speed and the 50-year recurrence extreme wind speed model (EWM) in

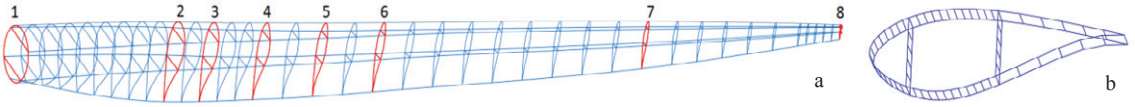

Figure 2: (a) the 38 blade sections and 8 airfoil profiles, in red. (b) a section of the meshed blade.

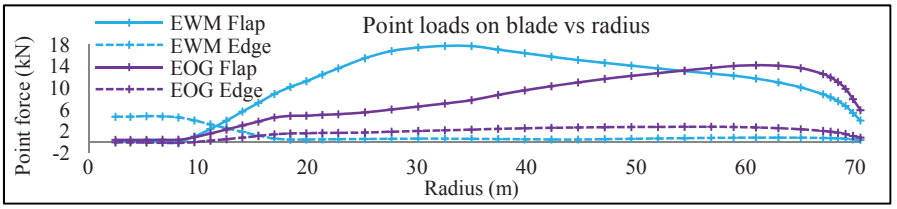

Figure 3: EWM and EOG edgewise and flapwise point forces along the blade span.

parked conditions [10]. The wind speeds in these cases were 19.61 and 70 m/s respectively. The EWM load case was performed with the blades fully pitched to 90° and included a yaw error of 15°. Figure 3 shows the distribution of edgewise and flapwise loads versus blade length for the two IEC cases.

6. Failure Criteria

Three failure criteria were specified for the design of this blade: (1) blade tip deflections do not violate the minimum distance between the blade tip and turbine tower, (2) material strains stay below their failure strain values, and (3) the blade withstands the critical buckling load.

6.1. Tip Deflection

The tip deflection criterion required that a minimum of 30% clearance of the static tower-to-tip distance be maintained for a turning rotor, and a 5% clearance for parked conditions [11]. The static, unloaded clearance was defined in [1] to be 12.09 m. Therefore, the maximum tip deflection during the rotating (EOG) and parked (EWM) load conditions was limited to 8.46 m and 11.48 m respectively.

6.2. Material Strains

The maximum and minimum strain criteria were used to verify that no elements in the model exceeded the design strains of the material. The material design strains were determined from the partial safety factors for the loads and the combined partial safety factors for the materials. The partial safety factor for the material based on short term (static) verification was found to be 2.205. This value was based on an analysis safety factor of 1.35 and reduction factors concerning the effect of aging and temperature and the resin infusion production method with a post cure [11]. The partial safety factor for aerodynamic loads was defined as 1.35 in [11] for normal and extreme loading conditions. Gravitational and other inertial forces (rotation) have a slightly lower safety factor but were both increased to 1.35 in this study to simplify the loading conditions, thus representing a conservative design methodology. The safety factor for loads and materials was calculated to be 2.977.

This study was concerned only with the strain of carbon fiber plies since they are stiffer than glass plies and exhibit a lower strain to failure. In reference [3], unidirectional carbon fiber mixed with 30% $\pm$45° glass fiber (by weight) was used for the spar flange layup: yielding a failure strain of 1.35% for

tension and -0.90% for compression. Due to the unavailability of failure strains for the carbon fiber material selected in this study, the same values have been applied here as those specified in [3]. Using these values and the safety factor of 2.977, the design strains for tension and compression were calculated as 0.453% and -0.302% respectively.

6.3. Buckling

The buckling study required a 1.634 safety factor, meaning that the structure must be capable of withstanding 1.634 times the worst case buckling condition. The safety factor for the stability analysis was based on an analysis safety factor of 1.35 and reduction factors to account for scattering of the moduli and temperature effects [11].

7. Design Method

The procedure used for defining the composite layup followed that presented by [5]: designing first for bending stiffness, then addressing buckling resistance. Bending stiffness was created by stacking up layers of carbon fiber with 0^o orientations to both the upper and lower spar flanges until both the tip deflection and material strain were above the acceptable failure criteria. Plies were added to the spar flanges one section at a time (starting at the root and moving outward) after which, the blade was re-submitted for analysis. The shear webs maintained a constant layup of $\pm 45_{glass}$/core/$\pm 45_{glass}$ with 0.004/0.040/0.004 m thicknesses respectively along the span.

Next, the airfoil shell was added to the model and buckling simulations were performed. $\pm 45^o$ symmetric layups were used for the airfoil skin along with a single 0^o glass fiber ply to reduce stress concentrations due to ply drops in the thin skin. In the regions fore and aft of the spar flanges, layers of core material were implemented in the skin layup to increase buckling resistance. Additional layers of $\pm 45^o$ plies were needed near the blade root to withstand the edgewise bending loads due to gravity. After a buckling analysis was performed, additional layers of $\pm 45^o$ plies were distributed in the failed regions, and the study was run again, until the critical load was above 1.634.

Fatigue studies were not performed, though edgewise fatigue likely does not present an issue due to the strict safety factors described above. In addition, the safety factor for edgewise fatigue (1.634), as presented in [3], was lower than that for static loads (2.977).

8. Results and Discussion

Table 2 presents the various analyses performed and their results. The EOG load case was found to produce the largest tip deflection and strain, while the EWM load case was the most severe in terms of the critical buckling load. As seen in Figure 3, the EWM has a larger total load than the EOG, suggesting why buckling is more critical here. The EOG has a higher load along the outer 26% of the blade length (52m and higher) where it is much more flexible. In fact, 62% of the blade tip deflection occurs in this region, explaining why this load case produces a higher deflection.

The blade position also played an effect on the results. Positions 1, 2, 3, and 4 in Table 2 refer to the following blade orientations respectively: pointing down, horizontal-rotating upwards, pointing up, horizontal-rotating downwards. Due to the available load cases studied by [1], it was not possible to perform an FE analysis applying the EWM load condition to the blades while in horizontal positions. This is because the EWM condition included a 15^o yaw error that does not affect a blade in the horizontal position in the same manner as it does to one in a vertical position.

Table 2: Simulation results. SF, LE, and TE refer to the spar flange, leading edge region, and trailing edge region of the blade.

Load Case	Results	Position 1	Position 2	Position 3	Position 4
EOG / / EWM	Tip flap deflection (m)	5.052 / / 4.723	5.072	**5.120** / /4.795	5.115
	Max strain (%)	0.198 / / 0.181, SF	**0.270, LE**	0.194 / / 0.176, SF	0.166, SF
	Min strain (-%)	0.167 / / 0.154, SF	**0.277, TE**	**0.170** / / 0.159, **SF**	0.169, SF
	Nonlin. crit. buckling load	2.005 / / 1.751	1.898	1.666 / / **1.659**	1.872

Quasi-static simulations including nonlinear geometries were performed to determine the maximum tip deflection and maximum and minimum strains. Shear strain, though never approaching critical values, was also monitored, with the largest values occurring in the shear webs.

The nonlinear critical buckling load studies were performed by using the modified Riks method, where both load magnitude and displacements were treated as unknowns [9]. Buckling first occurred in the spar flange (SF) for all load scenarios. Buckling was such a dominating condition that neither tip deflection nor max/min strain in the spar flanges came close to exceeding failure criteria. The critical strains were found in the leading (LE) and trailing edge (TE) regions near the root of the blade during a rotation upwards (against gravity).

Fig. 4 (a) shows the mass distribution of the final blade. This study yielded a thicker layup along most of the span because buckling was not considered in [1]. However, [1] is heavier near the root because it included the weight of the root connection while this study did not. Fig. 4 (b) is a plot of the strain along the length of the blade for the max/min spar strain load case. The spikes in the chart indicate ply drops. The large amplitude of these peaks and valleys is a bit unrealistic since the fiber plies would not actually represent an abrupt step change in thickness as has been done in the finite element model.

9. Further Optimization Techniques

After the blade withstood all failure conditions for both IEC load cases, weight reduction techniques were performed. Plies were removed from the root and tip regions of the blade moving inward until one of the failure criteria described above was met. Constraints were set in place so that no plies were allowed to have gaps along their length (ex. starting at one section, stopping, and starting again at a different section). This was done to keep manufacturing time down. Also, no more than two plies were allowed to start or stop at the same section in an effort to reduce stress concentrations due to ply drops. Finally, the layup was kept symmetric and balanced to assure no coupling developed.

It is recommended to distribute the 0^o and $\pm 45^o$ plies as evenly as possible throughout the thickness so that the laminate be more homogenous [12]. This strategy was adopted for this project, while other layup strategies were not studied. The results from weight the reduction steps were presented in Table 2 with

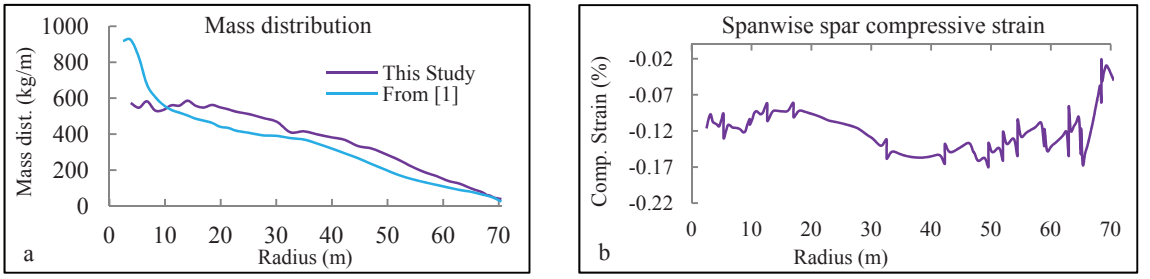

Figure 4: (a) mass distribution as a function of blade length. (b) compressive strain along the spar flange in compression.

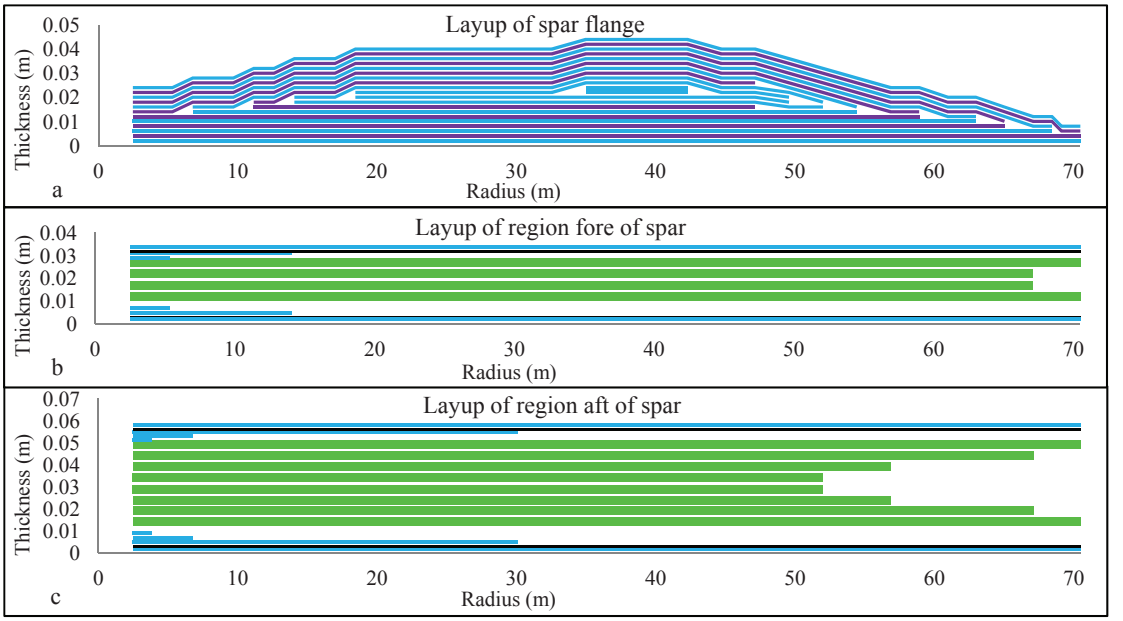

Figure 5: Ply layups of (a) the spar flanges, (b) the region on the fore side of the spar, and (c) the regions on the aft side of the spar. **Purple** lines represent 0^o carbon fiber, **blue** $\pm 45^o$ glass fiber, **black** 0^o glass fiber, and thick **green** lines represent core material.

the ply layups shown in Figure 5 (a-c). The blade weight was 24928 kg with the glass and carbon fiber plies accounting for 62.8% and 17.6% of the weight respectively. The core material weight was 14.4% of the total, while the lining and gel coat layers (not shown in Figure 5) represented 3.6% and 1.5%.

9.1. Sandwich Structures

In [13], studies were performed on 90 meter spars with and without a core material. The results showed an increase in critical buckling load of 31% when a 30 mm layer of core material was included in the center of the spar flanges. This reduced the number of $\pm 45^o$ anti-buckling plies required and yielded a weight reduction of 22%.

To determine if similar results could be obtained for the blade in this study, the same core layer was added to the spar flanges between r = 2.47 and 65 m. The goal was not to optimize the new sandwich structure blade, but to determine if there was potential for weight reduction.

The 30mm core layer added 1158 kg of weight, yielding a total mass increase of 4.3%. The maximum tip deflection and critical buckling load increased to 5.305 m and 2.247, representing increases of 5.7% and 36.8% respectively. The extra 36.8% of safety factor that was created in the critical buckling load suggests that a considerable amount of $\pm 45^o$ plies could be removed, thereby decreasing the weight.

9.2. Bend-twist Coupling

Another form of blade optimization comes in the form of adaptability. A blade that can adapt to the loading conditions can achieve an improved fatigue life and a higher efficiency. Many techniques exist for tailoring a blade in a passive manner so that it is capable of changing its shape, thus affecting its aerodynamics. One such method is to create a blade that exhibits bend-twist coupling [14] and [15].

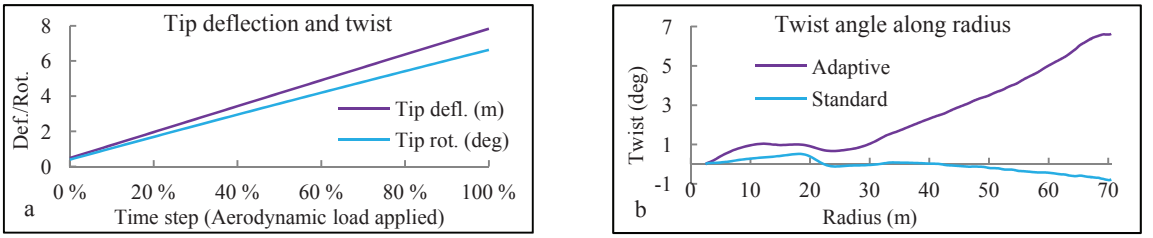

Figure 6: (a) behavior of blades as aerodynamic load increases. (b) tip twist for the adaptive and standard (from Table 2) blades.

A common method used in these references is to orient the 0^o fibers providing the bending stiffness to an angle between 20^o and 25^o to create an unbalanced composite. A final study was performed in which all carbon fibers in the optimized blade were rotated by 20 degrees to determine what passive twisting could be achieved with a simple fiber rotation. Figure 6 (b) shows the resulting twist (towards feather) of the coupled blade and the twist towards stall of the blade from Table 2. Bending stiffness significantly dropped yielding a tip deflection increase of 55% to 7.94 m. Blade weight remained constant, and the critical buckling load was within 1%. From this initial coupling study, the 6.6^o of twist indicates there is potential for improving performance by reducing extreme flap bending loads via bend-twist coupling.

10. Conclusions

A 70 m blade was designed to withstand the EOG and EWM load cases with material strains, tip deflection, and the critical buckling load used as failure criteria. The blade was designed by layering 0^o carbon fiber plies to achieve sufficient bending stiffness and $\pm 45^o$ glass fiber plies to contribute to buckling resistance. The airfoil skin and shear webs were created as sandwich structures, using glass fiber plies and a core material in regions other than the spar flanges. Based on this method, a composite ply layup definition was developed yielding a total blade weight of 24928 kg. Other techniques were introduced to determine potential for further blade optimization: namely the addition of core material in the spar flange regions, and load alleviation through bend-twist coupling. Future studies to be considered would be fatigue studies, flutter instability, and continued optimization.

11. References

[1] Frøyd L, Dahlhaug O. Rotor design for a 10 MW offshore wind turbine. ISOPE; Maui, USA, 2011.
[2] Jonkman J,Butterfield S,Musial W, Scott G. Definition of a 5-MW Reference Turbine for Offshore System Development. Tech. no. NREL/TP-500-38060. Golden, 2009. Web.
[3] Griffin, DA. Blade system design studies volume II: Preliminary blade designs and recommended test matrix, Kirkland: SAND2004-0073; 2004.
[4] Thomsen, O. "Sandwich Materials for Wind Turbine Blades.." Journal of Sandwich Structures and Materials 11 (2009): 7-26.
[5] Hoyland, Jorg. Challenges for large wind turbine blades. Thesis. Trondheim: NTNU, 2010. Print
[6] Joosse, PA, et al. Toward Cost Effective Large Turbine Components with Carbon Fibers. European Wind Energy Conference and Exhibition, Copenhagen. 2001.
[7] "Divinycell H - Technical data." Diabgroup.com. DIAB, Apr. 2011. Web.
[8] SolidWorks 2010. Concord, MA: Solidworks, 2010. Computer software.
[9] ABAQUS CAE. Vers. 6.10-2. Providence, RI, 2010. Computer software.
[10] IEC 61400-1, 2005. Wind turbines - Part 1: Design Requirements, Geneva: IEC 2005.
[11] Germanischer Lloyd, 2010. Guideline for the certification of wind turbines, Hamburg. 2010.
[12] Tsai, SW. Strength and Life of Composites. ISBN 978-0-9819143-0-5. 2008.
[13] Berggreen, C, Branner K, Jensen JF, Schultz JP. "Application and analysis of sandwich elements in the primary structure of large wind turbine blades." Journal of Sandwich Structures and Materials 9 (2007): 525-52. Print.
[14] Griffin DA. Evaluation of design concepts for adaptive wind turbine blades. SAND2002-2424. Kirkland: Sandia, 2002.
[15] Ong CH, Tsai SW. Design, manufacture and testing of a bend-twist D-spar. SAND 99-1324. Stanford, 1999. Print.